Int. J. Electrochem. Sci., 15 **(2020)** 4648 – 4659, doi: 10.20964/2020.05.82

International Journal of
ELECTROCHEMICAL
SCIENCE
www.electrochemsci.org

Enhanced performance of a PbO_2 electrocatalytic anode and its application for phenol oxidation

Xuefeng Wei[*], *Junjie Zhang, Juan Miao*[*], *Tingshuo Ji, Laiyang Zeng, Weiwei Lu*

College of Chemical Engineering & Pharmaceutics, Henan University of Science and Technology, Luoyang, 471023, P.R. China
[*]E-mail: xfwei@haust.edu.cn (X.W.), miaojuan@haust.edu.cn (J.M.)

Received: 1 January 2020 / *Accepted:* 2 March 2020 / *Published:* 10 April 2020

To enhance the electrocatalytic performance and stability of PbO_2 electrodes for the degradation of aqueous refractory organic pollutants, a sodium lauryl sulfonate (SLS)-modified PbO_2 electrode was prepared by a surfactant-assisted anodic electrodeposition method. The morphology, crystal phase, and electrocatalytic performance were studied by scanning electron microscopy (SEM), X-ray diffraction (XRD), linear sweep voltammetry (LSV) and phenol degradation. The stability and hydrophobicity of the PbO_2 anodes were investigated by accelerated life tests and contact angle measurements. The optimal SLS concentration is 120 mg/L in a bath solution during the electrode preparation process. The PbO_2-SLS-120 anode has an accelerated anode life of 72 h, which is 2.5 times longer than that of the undoped PbO_2 anode. The contact angle and oxygen evolution potential (OEP) of the PbO_2-SLS-120 anode are 102° and 1.54 V, respectively, which are larger than those of undoped PbO_2 anodes. It is suggested that PbO_2-SLS anode has good electrocatalytic performance due to the improvement of the electrode surface structure. Therefore, a PbO_2 anode with a simple and feasible preparation method was obtained with a good application prospect for the treatment of wastewater.

Keywords: electrocatalytic anode; lead dioxide; sodium lauryl sulfonate; hydrophobicity; phenol.

1. INTRODUCTION

The application of electrocatalytic oxidation technology in wastewater treatment is receiving increasing attention. It is environmentally friendly, efficient and compact because of its low production of secondary pollution, easy fabrication of the electrode, simple reactor configuration, and effective generation of reactive oxygen species (ROS) [1, 2]. The electrode material is clearly an important parameter in the electrochemical oxidation of organics, since the oxidation mechanisms vary on various kinds of anode. Among various electrocatalytic anodes, lead dioxide (PbO_2) anodes have the advantages of low cost, easy synthesis, high oxygen potential and corrosion resistance [3, 4]. PbO_2 is

an ideal anode material with strong mineralization ability for refractory organic compounds [5-7]. However, many aspects remain to be improved and developed. For example, compared with boron-doped diamond (BDD), the PbO_2 anode has lower electrocatalytic oxidation capacity [8]. The release of Pb^{2+} ions may cause secondary contamination if the coating is eroded during electrolysis [9]. Therefore, it is of great significance to further improve the catalytic property and stability of the PbO_2 anode.

Among the existing electrocatalytic anodes, the BDD anode has excellent electrocatalytic activity and stability [10-11]. A comparison of BDD and PbO_2 anodes shows that the surface adsorbability and hydrophilicity are important parameters that affect the performance of the anode [12-15]. In terms of the amount of hydroxyl radical (•OH), the PbO_2 anode produces more •OH than the BDD anode. However, in terms of the utilization of •OH, the PbO_2 anode is not as good as the BDD anode [16-19]. Regarding the hydrophilic surface of the PbO_2 anode, significantly more •OH is involved in the oxygen evolution reaction than in the oxidation of organic matter. However, the BDD anode shows hydrophobicity, and the oxidation efficiency of organic compounds is high due to its lower adsorption of •OH [20]. In short, the utilization ratio of •OH is related to its surface hydrophilicity. In consideration of the high production cost and high price due to the harsh preparation conditions of the BDD anode, the electrocatalytic performance of the PbO_2 anode can be reliably improved by regulating its hydrophilicity.

The change in hydrophobicity has been proven to affect the catalytic property and stability of the PbO_2 anode [21-25]. In recent years, various auxiliaries and materials have been added in the preparation process to regulate the hydrophilicity of the PbO_2 anode. In particular, different kinds of surfactants have been used to modify the anodes, such as polyethylene glycol (PEG), polyvinyl alcohol (PVA), bis(2-ethylhexyl) sulfosuccinate sodium salt (AOT) [26, 27], polyvinyl pyrrolidone (PVP) [27, 28], cetyltrimethyl ammonium bromide (CTAB) [22, 29], sodium dodecyl benzene sulfonate (SDBS) [30], and sodium dodecyl sulfate (SDS) [31].

Therefore, in the present work, sodium lauryl sulfonate ($C_{12}H_{25}SO_3Na$, SLS, M = 273), a typical and anionic surfactant, was adopted to modify the PbO_2 anode. This work aims to study the effects of SLS on the morphology and properties of the PbO_2 anode. The morphology and crystal structure were characterized by SEM and XRD, respectively. The electrocatalytic activity of the electrode was evaluated by phenol electrocatalytic degradation. In addition, stability of the electrode and surface hydrophilicity were tested by accelerated life experiments and contact angle measurements.

2. EXPERIMENTAL

2.1 Chemicals and materials

All chemicals were of analytical grade and obtained from Xilong chemical industry co. LTD, China. All aqueous solutions were prepared by deionized (DI) water (18.0 MΩ•cm) from a Millipore-

Q system. The porous titanium plate (thickness: 0.5 mm purity > 99.6%) were purchased from Baoji Tiecheng chemical equipment factory, China.

2.2 Electrodes preparation

A porous Ti substrate with dimensions of 2 cm ×3 cm × 0.5 mm was degreased in acetone and etched in a HCl and H_2O (volume ratio 1:2) mixture solution, followed by a thorough washing with DI water. A Sb-SnO_2 underlayer was modified on the Ti substrate using the sol-gel technique, which is modified from methods described by others [32, 33]. Then, an α-PbO_2 interlayer was loaded on Sb-SnO_2/Ti in a solution of 3.5 mol/L NaOH and 0.1 mol/L lead oxide with the applied current density of 3 mA/cm^2 for 1 h at 35 °C. The surface β-PbO_2 layer was coated on the α-PbO_2/Sb–SnO_2/Ti electrode through the surfactant-assisted anodic electrodeposition method. In this process, 100 mL solutions with 0.5 mol/L $Pb(NO_3)_2$, 0.05 mol/L NaF, 0.5 mol/L HNO_3 and certain amounts of SLS composite (0 mg/L, 30 mg/L, 60 mg/L, 90 mg/L, 120 g/L and 150 mg/L) were adopted as the deposition solution (marked as PbO_2-SLS-0, PbO_2-SLS-30, PbO_2-SLS-60, PbO_2-SLS-90, PbO_2-SLS-120, and PbO_2-SLS-150, respectively). The electrochemical deposition processes were performed at 65 °C for 1 h with the anodic current density of 20 mA/cm^2.

2.3 Characterization and performance tests

Scanning electron microscopy (SEM, Hitachi SU8020, Japan) was used to observe the morphology and elemental analysis. X-ray diffraction (XRD, BRUKER D8 Advance, German) using a Cu-Ka source (λ = 0.15416 nm) was adopted to analyse the crystal structure. The scanning angle (2θ) was 10-90°. Linear sweep voltammetry (LSV) was performed at an electrochemical workstation (CHI 660C, Shanghai Chenhua, China) in 0.5 mol/L H_2SO_4 solution in a three-electrode cell system. A platinum (Pt) sheet was used as the counter electrode, and Hg/Hg_2SO_4 (sat K_2SO_4) was used as the reference electrode. A contact anglemeter (SC-100, Dongguan Shengding Instrument Co. LTD, China) was employed to measure the contact angle of water on the electrode surface.

The accelerated lifetime tests were performed in 3 mol/L H_2SO_4 solution at the anode current density of 500 mA/cm^2 at 25 °C with a DC power supply (TPR-64100, Longwei Instruments Co., LTD, China). Variations in cell voltage were measured and recorded. The experiment stopped when the cell voltage had an increase of 5 V, and the time was defined as the accelerated life of the anode.

The electrochemical degradation phenol experiments were carried out in an undivided plexiglass cell equipped with a magnetic stirrer. The prepared PbO_2 anode (effective electrode area: 8 cm^2) was used as the working electrode, and a stainless-steel sheet with the same size was used as the counter electrode. The volume of phenol solution was 100 mL, and the initial phenol concentration was 100 mg/L. The electrode spacing was 1 cm, and 0.05 mol/L Na_2SO_4 was used as the electrolyte. Experiments were carried out at room temperature for 2 h at a current density of 5 mA/cm^2, which was provided by a DC power supply (2280-60-3, KEITHLEY, USA). The chemical oxygen demand (COD) values of samples were analysed every 0.5 h by a COD reactor (5B-1, Beijing Lianhua Science and Technology, China).

The instantaneous current efficiency (ICE) and energy consumption (Ep, kWh/gCOD) were calculated as follows [34, 35]:

$$ICE = \frac{(COD_{t_1} - COD_{t_2})}{8I(t_1 - t_2)} FV \quad (1)$$

$$Ep = \frac{UIt}{(COD_{t_1} - COD_{t_2})V} \quad (2)$$

where $CODt_1$ and $CODt_2$ are the values of COD at time t_1 and t_2, respectively; *F* is the Faraday constant (96,487 C/mol); *I* is the current (A); *t* is the electrolysis time; *U* is the cell voltage (V); *V* is the volume of the electrolyte (L).

3. RESULTS AND DISCUSSION

3.1 Surface morphology

Figure 1 shows the SEM images of the PbO_2 anodes prepared with different initial SLS concentrations. In Figure 1(a), the PbO_2 electrode without doping was rough with typical pyramidal shapes on the surface [36]. The particles varied in size, and some damages and cracks were found on the surface. In Figures 1(b-e), the surface morphology of electrode changed with the addition of the surfactant, i.e., the particles on the electrode surface were smaller and more compact with increasing SLS concentration. When the SLS concentration increased to 60 mg/L (Figure 1(c)), the number of particles with relatively smaller size increased. The electrode surface was uniform at the SLS concentration of 90 mg/L (Figure 1(d)), and good quality of PbO_2 coating with a compact and uniform structure was obtained at the SLS concentration of 120 mg/L (Figure 1(e)).

When we further increased the SLS concentration to 150 mg/L, the edges of the pyramid became indistinct, as shown in Figure 1(f). SLS is a typical surfactant. For one thing, the doping of a certain SLS concentration increased the nucleation rate of the PbO_2 crystal and inhibited the growth of crystal grain, so the crystal particle size decreased. For another, due to the coating effect of SLS, PbO_2 crystal particles were not easy to separate and aggregate. Therefore, uniform PbO_2 catalyst particles on the electrode surface were obtained. However, when the SLS concentration was too high, the mobility of PbO_2 particles decreased, which decreased the contact area between the PbO_2 thin film and the matrix and the adhesion, so the stability of the anode might decrease [30].

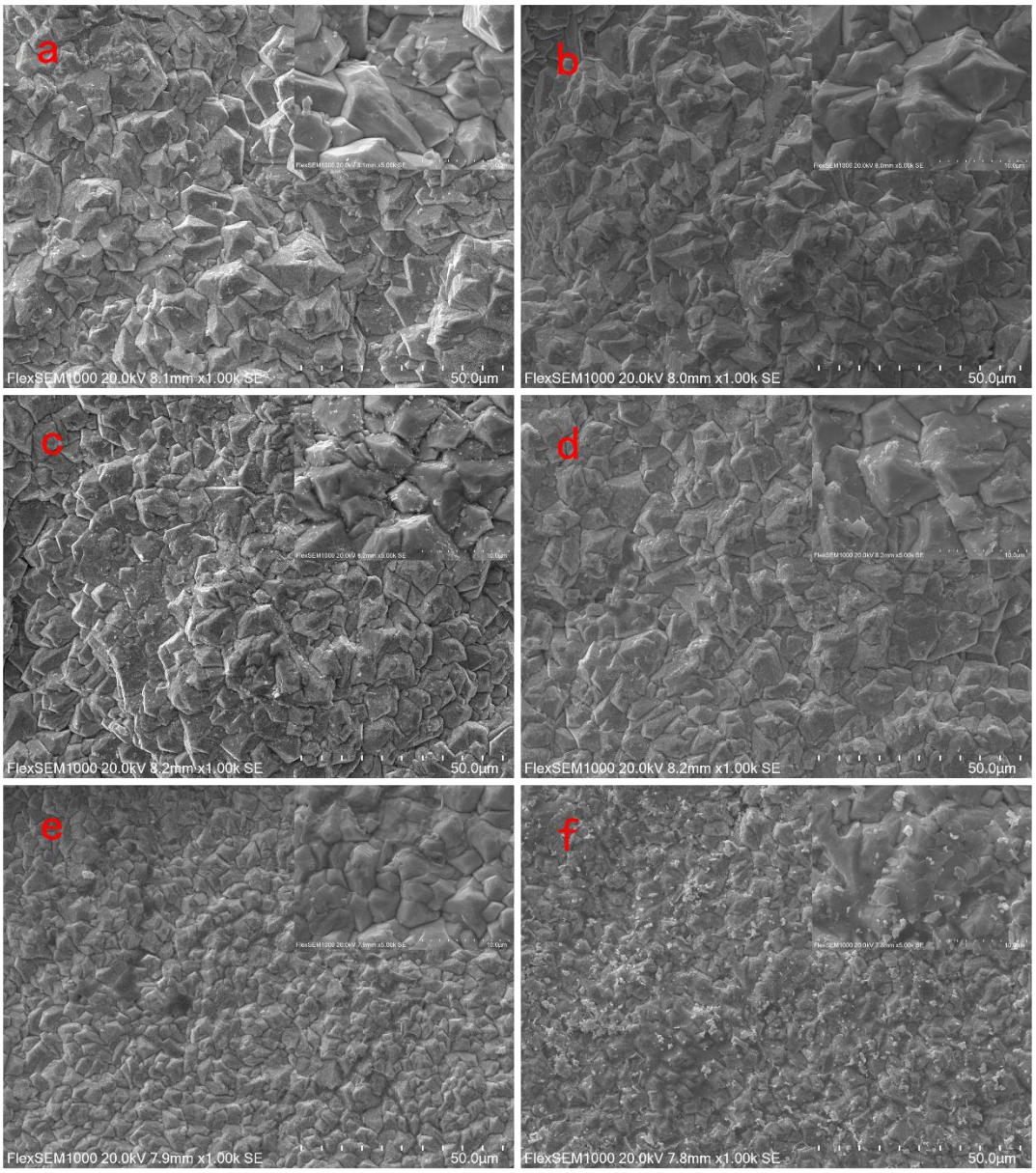

Figure 1. SEM images of (a) PbO_2-SDS-0, (b) PbO_2-SDS-30, (c) PbO_2-SD-60, (d) PbO_2-SDS-90, (e) PbO_2-SDS-120, and (f) PbO_2-SDS-150 anodes.

3.2 Structure of the PbO_2 anodes

XRD patterns of the six PbO_2 anodes are recorded in Figure 2, where diffraction peaks assigned to the (110), (101), (200), (211) and (301) of tetragonal β-PbO_2 (JCPDS 41-1492) are observed. The main crystalline phase of β-PbO_2 were maintained before and after the SLS doping. But the effects of SLS on different crystal planes of PbO_2 were imparity.When the conceration of SLS increased from 0 to 120 mg/L, the diffraction intensities of the (101) at $2\theta = 32.0°$ and (211) at $2\theta = 49.0°$ crystal planes increased, and the diffraction intensities of the (110) at $2\theta = 25.4°$ and (200) at $2\theta = 36.2°$ planes decreased. This result indicates that SLS molecules were more likely to cover the (110) and (200) planes and inhibit their growth. Meanwhile, PbO_2 crystals preferred to grow along with the

(101) and (211) crystal faces. Therefore, the diffraction intensities of the (101) and (211) planes were ehanced, as shown in the XRD patterns (II-VI). However, when excessive SLS was added, it covered all planes and greatly inhibited the crystal growth of PbO_2, resulting that all the diffraction intensities of the PbO_2-SlS-150 anode decreased, shown in the XRD patterns (VII). These results are consistent with the literature report [32]. The crystallite sizes of β-PbO_2 could be calculated according to Scherrer equation and the results are listed in Table 1. The average grain size of PbO_2 crystals on the PbO_2-SLS-120 electrode was smallest among the prepared anodes, which coincides with SEM analysis.

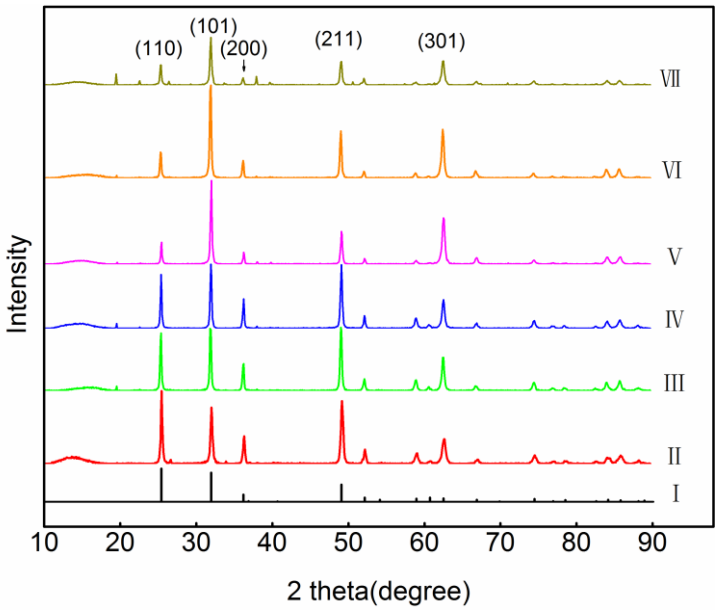

Figure 2. XRD patterns for PbO_2 (JCPDS 41-1492) (I), PbO_2-SLS-0 (II), PbO_2-SLS-30 (III), PbO_2-SLS-60 (IV), PbO_2-SLS-90 (V), PbO_2-SLS-120 (VI), and PbO_2-SLS-150 (VII) anodes.

Table 1. Average crystallite sizes of PbO_2 nanoparticles with different concentration of SLS.

Anodes	PbO_2-SLS-0	PbO_2-SLS-30	PbO_2-SLS-60	PbO_2-SLS-90	PbO_2-SLS-120	PbO_2-SLS-150
Average crystallite size/nm	34.6	33.4	33.8	32.3	31.1	32.4

3.3 Linear sweep voltammograms (LSV)

Figure 3 shows the LSV curves of the six prepared PbO_2 electrodes. Figure 3 shows that the oxygen evolution potential (OEP) of the PbO_2 electrodes were enhanced after the modification of SLS. Compared with that of the undoped PbO_2 anode (1.42 V), the OEP value of the PbO_2-SLS-120 electrode increased to 1.54 V. Generally, a high OEP value for the anode is desirable owing to the inhabitation of unwanted power loss on oxygen generation [37, 38]. Therefore, the PbO_2-SLS-120 with higher OEP indicates that it has a higher catalytic activity and potential for pollutant degradation.

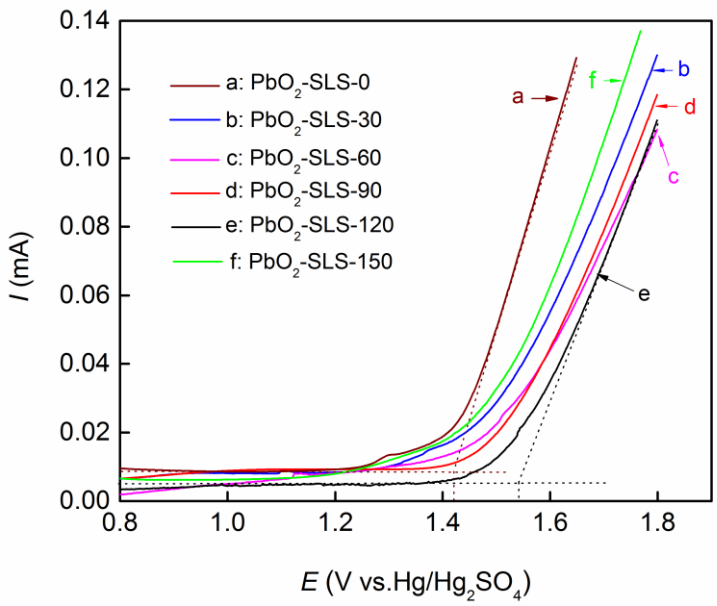

Figure 3. LSV curves of the (a) PbO-SLS-0, (b) PbO_2-SLS-30, (c) PbO_2-SLS-60, (d) PbO_2-SLS-90, (e) PbO_2-SLS-120, and (f) PbO_2-SLS-150 anodes in 0.5 mol/L H_2SO_4 solution with a scan rate of 1 mV/s at 25 °C.

3.4 Hydrophobic property

The contact angle is an important measure of the relationship between the reaction substance and the liquid wetting property. Figure 4 shows the contact angles of PbO_2 electrodes with different SLS doping. In Figure 4, the measured contact angles of PbO_2 without SLS doping was 31.4°. The contact angle increased from 34.1° to 102.3° with the increase in SLS concentration from 30 mg/L to 120 mg/L, which indicates that the SLS doping could improve the hydrophobicity of the PbO_2 electrode surface.

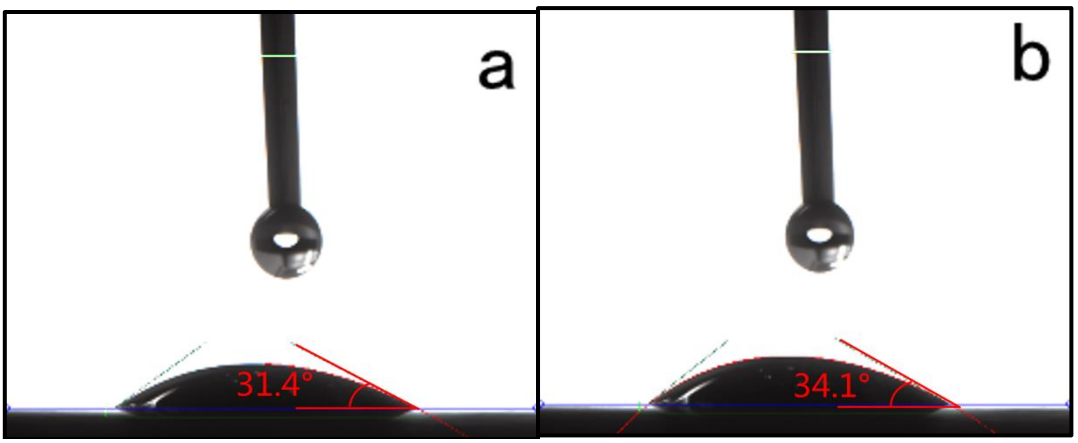

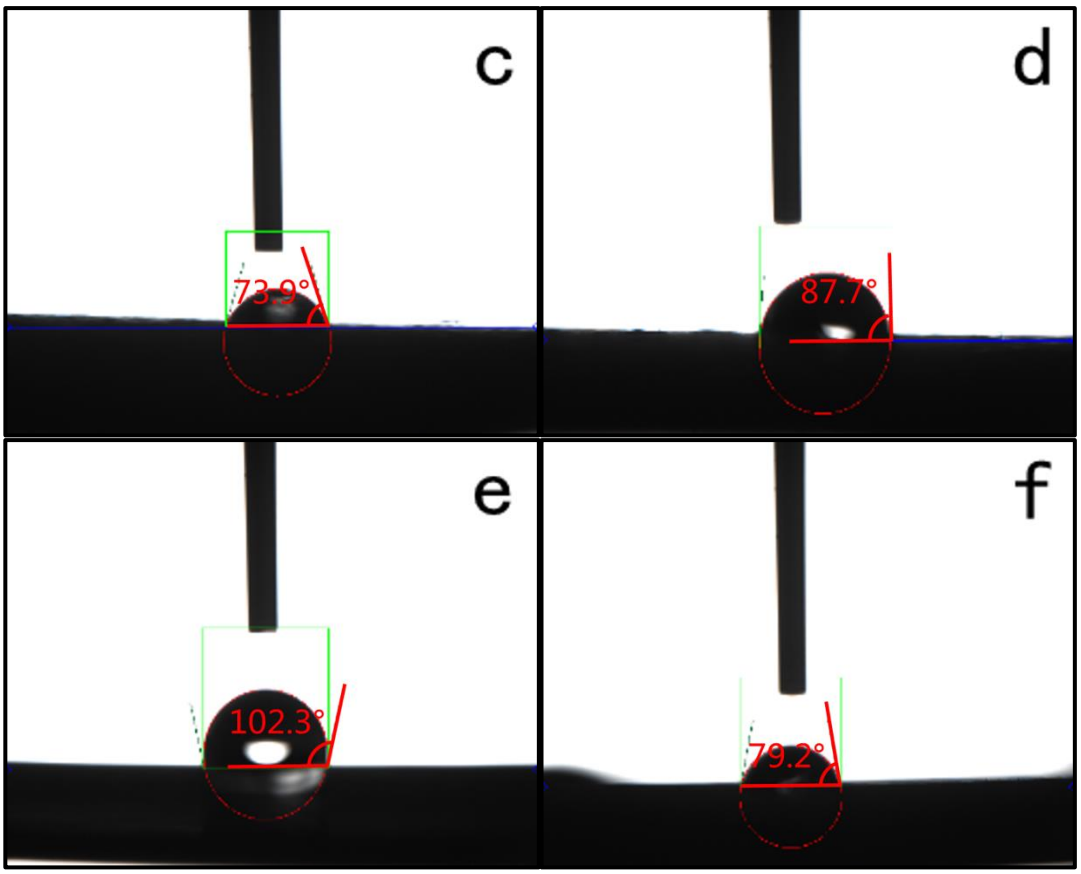

Figure 4. Contact angles of different PbO_2 anodes: (a) PbO_2-SLS-0, (b) PbO_2-SLS-30, (c) PbO_2-SLS-60, (d) PbO_2-SLS-90, (e) PbO_2-SLS-120, and (f) PbO_2-SLS-150.

According to previous studies [18, 23], the surface hydrophilicity of the anode could enhance the adsorption of •OH on the surface, so that most •OH did not participate in the reaction of organic matter in the solution. In contrast, due to the increase in hydrophobicity, •OH produced by the modified PbO_2 anode would accessed the electrolyte more, which was favourable for the oxidative degradation of organic compounds. The PbO_2-SLS-120 anode has the largest contact angle, i.e., the best hydrophobicity, which is conducive to increasing the free reactive oxygen species near the anode. Thus, the chance of reaction with organic matter was increased, and the degradation of organic contaminant would be enhanced. In addition, the PbO_2-SLS-150 anode has a relatively small contact angle possibly due to the change in surface morphology.

3.5 Electrochemical oxidation of phenol

To evaluate the electrochemical degradation activity of the PbO_2-SLS anodes, phenol was selected as the model pollutant for electrochemical oxidation. Figure 5 shows the COD removal efficiency on different PbO_2 anodes during the electrochemical degradation of phenol. In Figure 5, the COD removal on PbO_2 was enhanced after the SLS modification. The COD removal rate gradually increased with the increase in SLS concentration from 30 mg/L to 120 mg/L. The order of the COD

removal rate via different electrodes was PbO_2-SLS-120 > PbO_2-SLS-90 > PbO_2-SLS-60 > PbO_2-SLS-150 > PbO_2-SLS-30 > PbO_2-SLS-0 after 2 h electrolysis of phenol. However, when the SLS concentration increased to 150 mg/L, the mineralization rate of phenol decreased. The results are consistent with the XRD and SEM analysis, and the PbO_2-SLS-120 anode has the smallest grain size and the largest specific surface area, which provides the material basis for its good electrocatalytic properties. PbO_2-SLS-150 has lower COD removal than PbO_2-SLS-120, possibly due to excessive SLS, which made the pyramidal shape structure disappear. In addition, it could be explained by the LSV and contact angle experimental results. The anode with higher OEP and better hydrophobicity has good catalytic properties for phenol degradation due to fewer side reactions and abundant oxygen species. The ICE and Ep values of phenol oxidation on several PbO_2 anodes are shown in Table 2. The PbO_2-SLS-120 anode has higher current efficiency and lower energy consumption than other PbO_2 anodes. The value of ICE is higher and the value of Ep is lower for phenol oxidation than those values for the modified SnO_2 anodes, which were reported in our previous work [2].

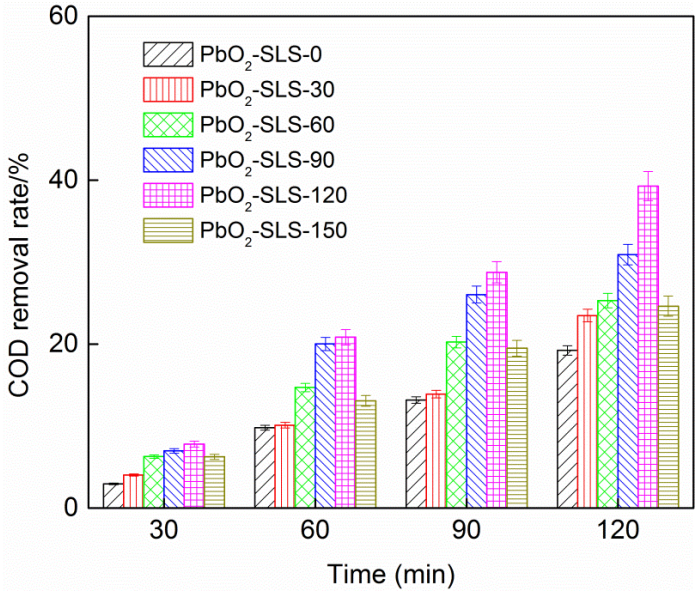

Figure 5. COD removal efficiency of phenol by (a) PbO_2-SLS-0, (b) PbO_2-SLS-30, (c) PbO_2-SLS-60, (d) PbO_2-SLS-90, (e) PbO_2-SLS-120, and (f) PbO_2-SLS-150 anodes in 0.05 mol/L Na_2SO_4 as supporting electrolyte after 2 h electrolysis, I = 5 mA/cm^2, and T = 25°C.

Table 2. ICE and Ep values obtained after 2 h of phenol degradation by different anodes; electrolyte: 0.05 mol/L Na_2SO_4, I = 5 mA/cm^2, T = 25 °C.

Anodes	PbO_2-SLS-0	PbO_2-SLS-30	PbO_2-SLS-60	PbO_2-SLS-90	PbO_2-SLS-120	PbO_2-SLS-150
ICE	0.080	0.230	0.224	0.327	0.389	0.262
Ep (kW/g)	0.183	0.064	0.065	0.045	0.038	0.056

3.6 Electrode stability evaluation

Electrode stability is also an important index to evaluate the electrode quality. Figure 6 presents the variation of cell voltage of these PbO_2 anodes under the accelerated life test condition. The SLS modification evidently enhanced the stability of the anode. The accelerated life of PbO_2-SLS-120 was longer than 72 h, which was approximately 2 times higher than that of PbO_2-SLS-0 (34 h). To assess the actual lifetime of the electrodes, an empirical relationship between the electrode service life (SL) and the current density (I) is used [39]:

$$SL \sim \frac{1}{I^n} \quad (3)$$

where n is 1.4-2.0. Assuming an average n of 1.7 for the PbO_2-SLS-120 anode, its service life could reach 55665 h in strong acidic solutions under the current density of 10 mA/cm^2. Therefore, the PbO_2-SLS-120 anode was sufficiently stable for application. However, the SLS-modified PbO_2 anode had a shorter accelerated life than some durable anodes, such as polyvinylidene-fluoride-modified PbO_2 (PbO_2-PVDF) electrode [33]. To further improve the service life of the electrode is a direction of our future work.

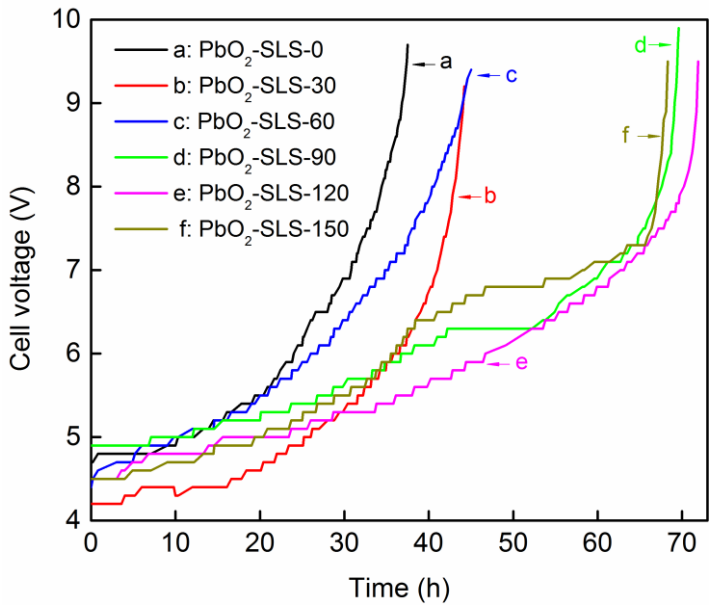

Figure 6. Accelerated life test comparison of the (a) PbO_2-SLS-0, (b) PbO_2-SLS-30, (c) PbO_2-SLS-60, (d) PbO_2-SLS-90, (e) PbO_2-SLS-120, and (f) PbO_2-SLS-150 anodes in 3 mol/L H_2SO_4 solution with a current density of 500 mA/cm^2 at 25 °C.

4. CONCLUSION

A PbO_2 electrode modified by the typical anionic surfactant sodium lauryl sulfonate (SLS) with good performance was prepared. The hydrophobicity of the PbO_2 anode was regulated by doping SLS,

which enhanced the catalytic activity and improved the stability of the anode due to its effect on the nucleation rate and growth direction of the PbO_2 crystal on the electrode surface. It was proven that the mineralization efficiency of the organic contaminant on the anode was related to the electrocatalytic activity and surface wettability of the anode. When the SLS concentration was 120 mg/L, the SLS-modified PbO_2 anode had an OEP of 1.54 V, a contact angle of 102.3°, and an accelerated life of 72 h, which were higher than those of other prepared PbO_2 anodes in this study. The PbO_2-SLS-120 anode could obtain a COD removal of approximately 40% for phenol degradation within 2 h, which shows an increased current efficiency and decreased energy consumption. Therefore, the PbO_2-SLS anode with simple preparation condition, low cost, and long service life has potential in industrial applications.

ACKNOWLEDGEMENTS
This work was supported by National Natural Science Foundation of China (21403058 and 21673067), and the Key Scientific Research Projects of Higher Education Institutions in Henan Province, China (20A610001).

References

1. Y. J. Feng and X. Y. Li, *Water Res*., 37(2003)2399.
2. Z. R. Sun, H. Zhang, X. F. Wei, R. Du and X. Hu, *J. Electrochem. Soc.*, 162 (2015)H590.
3. Y. Liu and H. Liu, *Electrochim. Acta*, 53(2008)5077.
4. W. Zhao, J. T. Xing, D. H. Chen, D.Y. Jin and J. Shen, *J. Electroanal. Chem.*, 775(2016)179.
5. Y. W. Yao, M. Y. Li, Y. Yang, L. L. Cui and L. Guo, *Chemosphere*, 216(2019)812-822.
6. C. Tan, B. Xiang, Y. J. Li, J. W. Fang and M. Huang. *Chem. Eng. J.*, 166(2011)15.
7. Y. Chen, H.Y. Li, W. J. Liu， Y. Tu, Y. H. Zhang, W. Q. Han and L. J. Wang. *Chemosphere*, 113(2014) 48.
8. L. S. Andrade, T. T. Tasso, R. C. Rocha, D. L. da Silva, R. C. Rocha, N. Bocchi and S. R. Biaggio, *Electrochim. Acta*, 54(2009) 2024.
9. D. Shao, J. D. Liang, X. M. Cui, H. Xu and W. Yan, *Chem. Eng. J.*, 244(2014)288.
10. X. M. Chen, F. R. Gao and G. H. Chen, *J. Appl. Electrochem.*, 35(2005)185.
11. H. Zazou, N. Oturan, Sonmez-Celebi, M. Hamdani and M. A. Oturan, *J. Electroanal. Chem.*, 774(2016)22.
12. M. Panizza and G. Cerisola, *Electrochim. Acta*, 48 (2003)3491.
13. M. Panizza and G. Cerisola, *Electrochim. Acta*, 49 (2004)3221.
14. M. Panizza and G. Cerisola, *Electrochim. Acta*, 51(2005)191.
15. I. Sires, E. Brillas, G. Cerisola and M. Panizza, *J. Electroanal. Chem.*, 613(2008)151.
16. X. P. Zhu, S. Shi, J. Wei, F. X. Lv, H. Z. Zhao, J. T. Kong, Q. He and J. R. Ni, *Environ. Sci. Technol.*, 41(2007)6541.
17. X. P. Zhu, M. Tong, S. Shi, H. Z. Zhao and J. R. Ni, *Environ. Sci. Technol.*, 42(2008)4914.
18. X. P. Zhu, J. R. Ni and P. Lai, *Water Res.*, 43(2009)4347.
19. F. Sopaj, M. A. Rodrigo, N. Oturan, F. I. Podvorica, J. Pinson and M. A. Oturan, *Chem. Eng. J.*, 262(2015)286.
20. G. H. Zhao, Y. G. Zhang, Y. Z. Lei, B. Y. Lv, J. X. Gao, Y. A. Zhang and D. M. Li, *Environ. Sci. Technol.*, 44(2010)1754.
21. X. Y. Duan, F. Ma, Z. X. Yuan, L. M. Chang and X. T. Jin, *Electrochim. Acta*, 76(2012)333.
22. X. Y. Duan, F. Ma, Z. X. Yuan, L. M. Chang and X. T. Jin, *J. Electroanal. Chem.*, 677(2012)90.
23. Y. P. He, X. Wang, W. Huang, R. Chen and H. Lin, *Chemosphere*, 193(2017)89.

24. J. Y. Chang and S. M. Park, *Electrochim. Acta*, 108(2013)86.
25. P. Z. Sun and D. H. Chen, *J. Rare Earths*, 34(2016)507.
26. W. H. Yang, W. T. Yang and X. Y. Lin, *Appl. Surf. Sci.*, 258(2012)5716.
27. F. Fu, W. H. Yang and C. Y. Ke, *Mater. Chem. Phys.*, 220(2018)155.
28. G. Darabizad, M. S. Rahmanifar, M. F. Mousavi and A. Pendashteh, *Mater. Chem. Phys.*, 156(2015)121.
29. B. Zhang, J. H. Zhong, Z. M. Cheng and H. G. Yang, *J. Electroanal. Chem.*, 689(2013)1.
30. X. Y. Duan, F. Xu, Y. Wang, Y. W. Chen and L. M. Chang, *Electrochim. Acta*, 282(2018)662.
31. X. L. Li, H. Xu and W. Yan, *J. Alloys Compd.*, 718(2017)386.
32. H. Lin, J. F. Niu, S. Y. Ding and L. L. Zhang, *Water Res.*, 46(2012)2281.
33. X. L. Li, H. Xu and W. Yan, *Appl. Surf. Sci.*, 389(2016)278.
34. M. Panizza, C. Bocca and G. Cerisola, *Water Res.*, 46(2012)2281.
35. S. Kumar, S. Singh, and V. C. Srivastava, *Chem. Eng. J.*, 263(2015)135.
36. H. Xu, D. Shao, Q. Zhang, H. H. Yang and W. Yan, *RSC Adv.*, 4(2014)25011.
37. Y. Chen, L. Hong, H. M. Xue, W. Q. Han, L. J. Wang, X. Y. Sun and J. S. Li, *J.Electroanal. Chem.*, 648(2010)119.
38. L. C. Zhang, L. Xu, J. He and J. J. Zhang, *Electrochim. Acta*, 117(2014)192.
39. M. H. Zhou, Q. Z. Dai, L. L. Lei, C. A. Ma and D. H. Wang, *Environ. Sci. Technol.*, 39(2005)363.